Transport in Porous Media (2021) 139:185–201
https://doi.org/10.1007/s11242-021-01649-4

Optimal Stability Thresholds in Rotating Fully Anisotropic Porous Medium with LTNE

Florinda Capone[1] · **Maurizio Gentile**[1] · **Jacopo A. Gianfrani**[1]

Received: 21 November 2020 / Accepted: 5 July 2021 / Published online: 29 July 2021

Abstract
The onset of thermal convection in an anisotropic horizontal porous layer heated from below and rotating about vertical axis, under local thermal non-equilibrium hypothesis is studied. Linear and nonlinear stability analysis of the conduction solution is performed. Coincidence between the linear instability and the global nonlinear stability thresholds with respect to the L^2—norm is proved.

Article Highlights

- **A necessary and sufficient condition for the onset of convection in a rotatinganisotropic porous layer has been obtained.**
- **It has been proved that convection can occur only through a steady motion.A detailed proof is reported thoroughly.**
- **Numerical analysis shows that permeability promotes convection, whilethermal conductivities and rotation stabilize conduction.**

Keywords Mechanical anisotropy · Thermal anisotropy · Thermal non-equilibrium · Rotating layer · Linear instability · Global nonlinear stability

1 Introduction

Over the years, thermal convection in porous media has attracted the interest of many researchers because numerous applications in geological context and in many engineering fields such as geothermal energy utilization, thermal insulation technology, tube refrigerators, heat exchangers, oil reservoir modelling and many others (see, for instance, Capone et al. 2020a; Gentile and Straughan 2013, 2017; Tyvand and Noland 2020; Barletta 2019; Straughan 2008; Nield and Bejan 2017; Capone and De Luca 2017; Capone and Rionero 2016b; Capone and De Luca 2014a, 2012 and references therein)

✉ Florinda Capone
fcapone@unina.it

[1] Dipartimento di Matematica e Applicazioni "R.Caccioppoli", Universitá degli Studi di Napoli Federico II, Via Cintia, 80126 Napoli, Italy

In nature, many porous media, like for example sedimentary and metamorphic rocks, exhibit a strong anisotropic behaviour in both thermal and mechanical features. Moreover, anisotropy is a property of artificial porous materials, as well, for example materials used in chemical engineering. Because of the emerging utilization of fully anisotropic porous materials in many applications to real life, the majority of investigations on thermal convection in porous media dealt with anisotropic porous materials (Malashetty et al. 2005; Tyvand and Storesletten 2015; Storesletten 2004; Capone et al. 2010, 2012; Nield and Kuznetsov 2019; Kuznetsov et al. 2015; Capone and De Luca 2020; Capone and Rionero 2016a; Storesletten and Rees 1997; Govender and Vadasz 2007).

Furthermore, as far as thermal convection in porous media is concerned, there are many situations in which local thermal equilibrium assumption is not realistic and therefore the fluid temperature, T_f, is supposed to be different from the solid skeleton temperature, T_s. When the two temperatures are different the scheme is usually referred to as local thermal non-equilibrium scheme, namely LTNE. In LTNE scheme, it is assumed that fluid and solid phases communicate in such a way that heat exchanges better describe the physics of the problem. In the past as nowadays, a great attention to LTNE flows in porous media is given by many researchers, as shown in Capone and Gentile (2018), Capone et al. (2020a, b), Govender and Vadasz (2007), Straughan (2013), Barletta and Rees (2015), Kuznetsov et al. (2015), Celli et al. (2017), Franchi et al. (2018), Hema et al. (2020). This is due to the numerous applications to real-life situations, such as preserving food, cooling computer chips, nanofluids flows, biological tissues analysis and convection in stellar atmospheres.

In the present paper, we analyse the onset of convection in a fully anisotropic porous medium in LTNE scheme, allowing for the Corolis force. The study of flow in rotating porous medium is motivated by its numerous applications in real processes, like, for example, in physiological processes in human body subject to rotating trajectories; in engineering processes with rotating electronic devices, in magma flow in the Earth mantle close to the Earth crust and in chemical process industry (Vadasz 1998, 2002, 2016, 2019; Govender 2007; Capone et al. 2020a, b; Capone and De Luca 2014b).

The plan of the paper is the following. In Sect. 2, we introduce the mathematical model and the dimensionless evolution equations for perturbation fields to conduction solution in order to study the stability of the motionless state (conduction solution). Then, in Sect. 3, a detailed proof of principle of exchange of stabilities is performed and the critical Rayleigh number for the onset of (stationary) convection is determined, in a closed algebraic form. Section 4 deals with the nonlinear stability analysis of the conduction solution and we prove the coincidence between the linear instability threshold and the (global) nonlinear stability threshold of the conduction solution, with respect to the L^2–norm. Finally, in Sect. 5, numerical simulations concerning the influence of rotation and anisotropy on the stability/instability thresholds is analysed.

2 Mathematical Model

Let us consider a horizontal porous layer of depth d, filled by an incompressible, homogeneous fluid at rest. We assume that the medium is uniformly heated from below and uniformly rotating about the vertical axis z (upward vertical) with constant angular velocity Ω. Let T_L be the temperature of the lower plane $z = 0$ and let T_U be the temperature of the upper plane $z = d$. In the local thermal non-equilibrium scheme (LTNE), denoting by T_f

and T_s the fluid temperature and the solid skeleton temperature, respectively, it turns out that

$$T_s = T_f = T_L \quad \text{on } z = 0, \qquad T_s = T_f = T_U \quad \text{on } z = d \quad (T_L > T_U)\,. \tag{1}$$

Moreover, we assume that the layer is anisotropic and we denote by $\mathcal{K}$ the permeability tensor, and let $\mathcal{D}_s$, $\mathcal{D}_f$ be the thermal conductivity tensors of solid phase and fluid phase, respectively. Assume that the principal axis (x, y, z) of the permeability tensor are the same as the ones of conductivity tensor, one obtains

$$\begin{aligned}
&\mathcal{K} = K_z \mathcal{K}^* \qquad \mathcal{K}^* = \begin{pmatrix} \xi_1 & 0 & 0 \\ 0 & \xi_2 & 0 \\ 0 & 0 & 1 \end{pmatrix} \qquad \xi_1 = \frac{K_x}{K_z} \quad \xi_2 = \frac{K_y}{K_z} \\
&\mathcal{D}_s = \kappa_z^s \mathcal{D}_s^* \qquad \mathcal{D}_s^* = \begin{pmatrix} \zeta_1 & 0 & 0 \\ 0 & \zeta_2 & 0 \\ 0 & 0 & 1 \end{pmatrix} \qquad \zeta_1 = \frac{\kappa_x^s}{\kappa_z^s} \quad \zeta_2 = \frac{\kappa_y^s}{\kappa_z^s} \\
&\mathcal{D}_f = \kappa_z^f \mathcal{D}_f^* \qquad \mathcal{D}_f^* = \begin{pmatrix} \eta & 0 & 0 \\ 0 & \eta & 0 \\ 0 & 0 & 1 \end{pmatrix} \qquad \eta = \frac{\kappa_h^f}{\kappa_z^f}
\end{aligned} \tag{2}$$

where, in particular, η is the thermal anisotropy parameter for the fluid phase.

The mathematical model, in the Oberbeck–Boussinesq approximation and accounting for the Coriolis force due to the uniform rotation of the layer about the vertical axis z is (Straughan 2015; Govender and Vadasz 2007; Capone and Gentile 2018; Capone et al. 2020a)

$$\begin{cases}
\mathbf{v} = \mu^{-1}\mathcal{K}\left[-\nabla p + \rho_f g \alpha T_f \mathbf{k} - \dfrac{2\Omega\rho_f}{\varepsilon}\mathbf{k}\times\mathbf{v}\right] \\
\nabla\cdot\mathbf{v} = 0 \\
\varepsilon(\rho c)_f T_{,t}^f + (\rho c)_f \mathbf{v}\cdot\nabla T_f = \varepsilon\nabla\cdot(\mathcal{D}^f\cdot\nabla T_f) + h(T_s - T_f) \\
(1-\varepsilon)(\rho c)_s T_{,t}^s = (1-\varepsilon)\nabla\cdot(\mathcal{D}^s\cdot\nabla T_s) - h(T_s - T_f)
\end{cases} \tag{3}$$

where $\mathbf{v}$, p, T_s and T_f are (seepage) velocity, reduced pressure, solid phase temperature and fluid phase temperature, respectively; μ, ρ_f, ρ_s, g, α, Ω, ε, c, h are dynamic viscosity, fluid density, solid density, gravity acceleration, thermal expansion coefficient, angular velocity, porosity, specific heat and interaction coefficient, respectively.

To system (3), we append the following boundary conditions

$$\begin{aligned}
&T_s = T_f = T_L \quad \text{on } z = 0, \qquad T_s = T_f = T_U \quad \text{on } z = d, \\
&\mathbf{v}\cdot\mathbf{n} = 0 \quad \text{on } z = 0, d
\end{aligned} \tag{4}$$

being $\mathbf{n}$ the unit outward normal to planes $z = 0, d$.

The system (3) admits the conduction solution m_0:

$$m_0 = \left\{ \bar{\mathbf{v}} = \mathbf{0}\,, \quad \bar{T}_s = \bar{T}_f = -\beta z + T_L\,, \quad \bar{p} = -\rho_f g\alpha\beta\frac{z^2}{2} + \rho_f g\alpha T_L z \right\} \tag{5}$$

where $\beta = \dfrac{T_L - T_U}{d} (> 0)$ is the adverse temperature gradient.

In order to study the stability of the steady solution (5), let us introduce the following perturbation fields

$$v_i = u_i + \bar{v}_i \qquad T_s = \phi + \bar{T}_s \qquad T_f = \theta + \bar{T}_f \qquad p = \pi + \bar{p} \tag{6}$$

and the dimensionless quantities

$$x_i = \tilde{x}_i d, \quad t = \tilde{t}\frac{\varepsilon d}{U}, \quad \pi = \tilde{\pi} P, \quad u_i = \tilde{u}_i U, \quad \theta = \tilde{\theta} T', \quad \phi = \tilde{\phi} T' \tag{7}$$

where

$$U = \frac{\varepsilon \kappa_z^f}{(\rho c)_f d}, \qquad P = \frac{U \mu d}{K_z}, \qquad T' = \beta d \sqrt{\frac{\kappa_z^f \varepsilon \mu}{\beta g \alpha K_z \rho_f^2 c_f d^2}}. \tag{8}$$

The dimensionless equations for the perturbation fields, omitting all the tilde, are

$$\begin{cases} \mathcal{K}^{-1}\mathbf{u} = -\nabla \pi + R\theta \mathbf{k} - \mathcal{T}\mathbf{k} \times \mathbf{u} \\ \nabla \cdot \mathbf{u} = 0 \\ \theta_{,t} + \mathbf{u} \cdot \nabla \theta = Rw + \eta \Delta_1 \theta + \theta_{,zz} + H(\phi - \theta) \\ A\phi_{,t} - \zeta_1 \phi_{,xx} - \zeta_2 \phi_{,yy} - \phi_{,zz} + H\gamma(\phi - \theta) = 0 \end{cases} \tag{9}$$

where $\Delta_1 = \partial_{,xx} + \partial_{,yy}$ and

$$\gamma = \frac{\varepsilon \kappa_z^f}{(1-\varepsilon)\kappa_z^s}, \qquad A = \frac{(\rho c)_s \kappa_z^f}{(\rho c)_f \kappa_z^s}, \qquad H = \frac{hd^2}{\varepsilon \kappa_z^f}$$

$$R^2 = \frac{K_z \rho_f^2 c_f d^2 \beta g \alpha}{\mu \varepsilon \kappa_z^f} \quad \text{Rayleigh number}, \qquad \mathcal{T} = \frac{2\Omega \rho_f K_z}{\varepsilon \mu} \quad \text{Taylor number}.$$

To system (9), we append the following initial conditions

$$\mathbf{u}(\mathbf{x}, 0) = \mathbf{u}_0(\mathbf{x}), \quad \pi(\mathbf{x}, 0) = \pi_0(\mathbf{x}), \quad \theta(\mathbf{x}, 0) = \theta_0(\mathbf{x}), \quad \phi(\mathbf{x}, 0) = \phi_0(\mathbf{x}) \tag{10}$$

where $\nabla \cdot \mathbf{u}_0 = 0$, and the following boundary conditions

$$w = \theta = \phi = 0 \qquad \text{on } z = 0, 1. \tag{11}$$

We assume that perturbation fields are periodic in x and y directions of periods $\frac{2\pi}{a_x}$ and $\frac{2\pi}{a_y}$, respectively, and they belong to $W^{2,2}(V)$, $\forall t \in \mathbb{R}^+$where $V = \left[0, \frac{2\pi}{a_x}\right] \times \left[0, \frac{2\pi}{a_y}\right] \times [0, 1]$ is the periodicity cell. Then we denote by $(\cdot, \cdot)$ and $\|\cdot\|$ the scalar product on the Hilbert space $L^2(V)$, and the related norm, respectively.

3 Instability Analysis of m_0

In order to study the linear stability of m_0, let us consider the linear version of (9), i.e.

$$\begin{cases} \mathcal{K}^{-1}\mathbf{u} = -\nabla\pi + R\theta\mathbf{k} - \mathcal{T}\mathbf{k}\times\mathbf{u} \\ \nabla\cdot\mathbf{u} = 0 \\ \theta_{,t} = Rw + \eta\Delta_1\theta + \theta_{,zz} + H(\phi-\theta) \\ A\phi_{,t} - \zeta_1\phi_{,xx} - \zeta_2\phi_{,yy} - \phi_{,zz} + H\gamma(\phi-\theta) = 0 \end{cases} \tag{12}$$

under the boundary conditions (11). Applying the curl to $(12)_1$, one obtains

$$\begin{cases} w_{,y}\xi_2 - v_{,z} = R\theta_{,y}\xi_2 + \mathcal{T}u_{,z}\xi_2 \\ u_{,z} - w_{,x}\xi_1 = -R\theta_{,x}\xi_1 + \mathcal{T}v_{,z}\xi_1 \\ v_{,x}\xi_1 - u_{,y}\xi_2 = \mathcal{T}\xi_1\xi_2 w_{,z} \end{cases} \tag{13}$$

and deriving $(13)_1$ by y, $(13)_2$ by x and $(13)_3$ by z, one gets

$$\begin{cases} w_{,yy}\xi_2 - v_{,zy} = R\theta_{,yy}\xi_2 + \mathcal{T}u_{,zy}\xi_2 \\ u_{,zx} - w_{,xx}\xi_1 = -R\theta_{,xx}\xi_1 + \mathcal{T}v_{,zx}\xi_1 \\ v_{,xz}\xi_1 - u_{,yz}\xi_2 = \mathcal{T}\xi_1\xi_2 w_{,zz}. \end{cases} \tag{14}$$

Subtracting $(14)_2$ from $(14)_1$ and then substituting the result in $(14)_3$, it follows that

$$\xi_1 w_{,xx} + \xi_2 w_{,yy} + w_{,zz} = \xi_1 R\theta_{,xx} + \xi_2 R\theta_{,yy} - \mathcal{T}^2\xi_1\xi_2 w_{,zz}. \tag{15}$$

Let us consider now the autonomous system

$$\begin{cases} \xi_1 w_{,xx} + \xi_2 w_{,yy} + w_{,zz} + \mathcal{T}^2\xi_1\xi_2 w_{,zz} - \xi_1 R\theta_{,xx} - \xi_2 R\theta_{,yy} = 0 \\ \theta_{,t} - Rw - \eta\Delta_1\theta - \theta_{,zz} - H(\phi-\theta) = 0 \\ A\phi_{,t} - \zeta_1\phi_{,xx} - \zeta_2\phi_{,yy} - \phi_{,zz} + H\gamma(\phi-\theta) = 0 \end{cases} \tag{16}$$

and seek for solutions having the following time-dependence (Chandrasekhar 2013) $\hat{\varphi}(t,\mathbf{x}) = \varphi(\mathbf{x})\, e^{\sigma t}$, $\forall\hat{\varphi}\in(w,\theta,\phi)$, $\sigma\in\mathbb{C}$, (16) becomes

$$\begin{cases} \xi_1 w_{,xx} + \xi_2 w_{,yy} + w_{,zz} + \mathcal{T}^2\xi_1\xi_2 w_{,zz} - \xi_1 R\theta_{,xx} - \xi_2 R\theta_{,yy} = 0 \\ \sigma\theta - Rw - \eta\Delta_1\theta - \theta_{,zz} - H(\phi-\theta) = 0 \\ A\sigma\phi - \zeta_1\phi_{,xx} - \zeta_2\phi_{,yy} - \phi_{,zz} + H\gamma(\phi-\theta) = 0. \end{cases} \tag{17}$$

Let us multiply $(17)_1$ by w^*, $(17)_2$ once by $\xi_1\theta^*_{,xx}$ and once by $\xi_2\theta^*_{,yy}$, $(17)_3$ once by $\xi_1\phi^*_{,xx}$ and once by $\xi_2\phi^*_{,yy}$ where the asterisks denote the complex conjugate, accounting for the boundary conditions one obtains:

$$
\begin{aligned}
&\sigma\left[\xi_1\|\theta_{,x}\|^2+\xi_2\|\theta_{,y}\|^2+\frac{A\xi_1}{\gamma}\|\phi_{,x}\|^2+\frac{A\xi_2}{\gamma}\|\phi_{,y}\|^2\right]\\
&\quad=-\xi_1\|w_{,x}\|^2-\xi_2\|w_{,y}\|^2-(1+\mathcal{T}^2\xi_1\xi_2)\|w_{,z}\|^2-\xi_1R\left[(\theta_{,xx},w^*)+(w,\theta^*_{,xx})\right]\\
&\qquad-\xi_2R\left[(\theta_{,yy},w^*)+(w,\theta^*_{,yy})\right]-\xi_1\eta\|\theta_{,xx}\|^2-\xi_1\eta\|\theta_{,xy}\|^2-\xi_1\|\theta_{,xz}\|^2\\
&\qquad-H\xi_1\left[(\phi_{,xx},\theta^*)+(\theta,\phi^*_{,xx})\right]-H\xi_1\|\theta_{,x}\|^2-\xi_2\eta\|\theta_{,xy}\|^2-\xi_2\eta\|\theta_{,yy}\|^2\\
&\qquad-\xi_2\|\theta_{,yz}\|^2-H\xi_2\left[(\phi_{,yy},\theta^*)+(\theta,\phi^*_{,yy})\right]-H\xi_2\|\theta_{,y}\|^2-\frac{\zeta_1\xi_1}{\gamma}\|\phi_{,xx}\|^2\\
&\qquad-\frac{\zeta_2\xi_1}{\gamma}\|\phi_{,xy}\|^2-\frac{\xi_1}{\gamma}\|\phi_{,xz}\|^2-H\xi_1\|\phi_{,x}\|^2-\frac{\zeta_1\xi_2}{\gamma}\|\phi_{,xy}\|^2\\
&\qquad-\frac{\zeta_2\xi_2}{\gamma}\|\phi_{,yy}\|^2-\frac{\xi_2}{\gamma}\|\phi_{,yz}\|^2-H\xi_2\|\phi_{,y}\|^2
\end{aligned}
\tag{18}
$$

and hence, since terms in (18) are real, then necessarily $\sigma\in\mathbb{R}$. Therefore, *the strong form of the principle of exchange of stabilities holds*, i.e. convection can occur only through a steady motion.

In order to determine the critical Rayleigh number for the onset of convection, by virtue of the principle of exchange of stabilities, setting $\sigma=0$ in (17), one obtains

$$
\begin{cases}
\xi_1 w_{,xx}+\xi_2 w_{,yy}+w_{,zz}+\mathcal{T}^2\xi_1\xi_2 w_{,zz}=\xi_1R\theta_{,xx}+\xi_2R\theta_{,yy}\\
\eta\Delta_1\theta+\theta_{,zz}-H\theta=-Rw-H\phi\\
\zeta_1\phi_{,xx}+\zeta_2\phi_{,yy}+\phi_{,zz}-H\gamma\phi=-H\gamma\theta.
\end{cases}
\tag{19}
$$

Denoting

$$
\begin{aligned}
&\mathcal{L}\equiv\xi_1\partial_{,xx}+\xi_2\partial_{,yy}+\partial_{,zz}+\mathcal{T}^2\xi_1\xi_2\partial_{,zz}\\
&\mathcal{L}_1\equiv\eta\Delta_1\theta+\partial_{,zz}-H\\
&\mathcal{L}_2\equiv\zeta_1\partial_{,xx}+\zeta_2\partial_{,yy}+\partial_{,zz}-H\gamma
\end{aligned}
\tag{20}
$$

(19) becomes

$$
\begin{cases}
\mathcal{L}w=\xi_1R\theta_{,xx}+\xi_2R\theta_{,yy}\\
\mathcal{L}_1\theta=-Rw-H\phi\\
\mathcal{L}_2\phi=-H\gamma\theta.
\end{cases}
\tag{21}
$$

Now, applying the operators $\mathcal{L}$ and $\mathcal{L}_2$ to $(21)_2$ and substituting $(21)_1$ and $(21)_3$ in the resulting equation, one leads

$$
\mathcal{L}\mathcal{L}_1\mathcal{L}_2\theta=-R^2\xi_1(\mathcal{L}_2\theta)_{,xx}-R^2\xi_2(\mathcal{L}_2\theta)_{,yy}+H^2\gamma\mathcal{L}\theta.
\tag{22}
$$

Splitting the operators $\mathcal{L}_1$ and $\mathcal{L}_2$, from (22) it follows that

$$
\begin{aligned}
&(\zeta_1\partial_{,xx}+\zeta_2\partial_{,yy}+\partial_{,zz}-H\gamma)(\eta\Delta_1+\partial_{,zz})\mathcal{L}\theta\\
&\quad=(\zeta_1\partial_{,xx}+\zeta_2\partial_{,yy}+\partial_{,zz})H\mathcal{L}\theta\\
&\qquad-R^2(\xi_1\partial_{,xx}+\xi_2\partial_{,yy})(\zeta_1\partial_{,xx}+\zeta_2\partial_{,yy}+\partial_{,zz})\theta\\
&\qquad+R^2(\xi_1\partial_{,xx}+\xi_2\partial_{,yy})H\gamma\theta.
\end{aligned}
\tag{23}
$$

By virtue of the periodicity and of the boundary conditions $(11)_2$, since the sequence $\{\sin(n\pi z)\}_{n\in\mathbb{N}}$ is a complete orthogonal system for $L^2([0,1])$, accounting for solutions of the form $\theta=\Theta_0\sin(n\pi z)e^{i(a_x x+a_y y)}$, (23) becomes

$$
\begin{aligned}
&(-\zeta_1a_x^2-\zeta_2a_y^2-n^2\pi^2-H\gamma)(-\eta a_x^2-\eta a_y^2-n^2\pi^2)\\
&(-\xi_1a_x^2-\xi_2a_y^2-n^2\pi^2-\mathcal{T}^2\xi_1\xi_2n^2\pi^2)\\
&\quad=(-\zeta_1a_x^2-\zeta_2a_y^2-n^2\pi^2)H(-\xi_1a_x^2-\xi_2a_y^2-n^2\pi^2-\mathcal{T}^2\xi_1\xi_2n^2\pi^2)\\
&\qquad-R^2(-\xi_1a_x^2-\xi_2a_y^2)(-\zeta_1a_x^2-\zeta_2a_y^2-n^2\pi^2-H\gamma).
\end{aligned}
\tag{24}
$$

Setting $A^*=1+\mathcal{T}^2\xi_1\xi_2$ and

$$
\begin{aligned}
f(a_x^2,a_y^2,n^2)=&\frac{\xi_1a_x^2+\xi_2a_y^2+n^2\pi^2A^*}{\xi_1a_x^2+\xi_2a_y^2}\\
&\cdot\left[\eta a_x^2+\eta a_y^2+n^2\pi^2+\frac{H(\zeta_1a_x^2+\zeta_2a_y^2+n^2\pi^2)}{\zeta_1a_x^2+\zeta_2a_y^2+n^2\pi^2+H\gamma}\right],
\end{aligned}
\tag{25}
$$

from (24) it follows that the critical Rayleigh number R_L for the onset of convection is given by

$$
R_L=\min_{(n^2,a_x^2,a_y^2)\in\mathbb{N}\times\mathbb{R}^+\times\mathbb{R}^+}f(a_x^2,a_y^2,n^2)
\tag{26}
$$

and since $f(a_x^2,a_y^2,n^2)$ is strictly increasing with n^2, this implies that the minimum is attained at $n^2=1$. Hence,

$$
R_L=\min_{(a_x^2,a_y^2)\in\mathbb{R}^+\times\mathbb{R}^+}f(a_x^2,a_y^2,1).
\tag{27}
$$

Remark 1 Define

$$
R_0=\frac{R_L}{\pi^2}=\min_{(\bar{x},\bar{y})\in\mathbb{R}^+\times\mathbb{R}^+}f_1(\bar{x},\bar{y}),
\tag{28}
$$

where

$$
\begin{aligned}
f_1(\bar{x},\bar{y})=&\frac{\xi_1\bar{x}+\xi_2\bar{y}+A^*}{\xi_1\bar{x}+\xi_2\bar{y}}\left[\eta\bar{x}+\eta\bar{y}+1+\frac{H_0(\zeta_1\bar{x}+\zeta_2\bar{y}+1)}{\zeta_1\bar{x}+\zeta_2\bar{y}+1+H_0\gamma}\right]\\
\bar{x}=&\frac{a_x^2}{\pi^2},\qquad\bar{y}=\frac{a_y^2}{\pi^2},\qquad H_0=\frac{H}{\pi^2}.
\end{aligned}
\tag{29}
$$

Let us observe that:

(i) In the case of horizontal isotropy, i.e. $\xi_1 = \xi_2$ and $\zeta_1 = \zeta_2$, the critical Rayleigh number R_0 given by (28) coincides with that one obtained in Capone and Gentile (2018);
(ii) In the absence of rotation ($\mathcal{T}^2 = 0$) and if the porous medium is isotropic ($\xi_1 = \xi_2 = \zeta_1 = \zeta_2 = \eta = 1$), then the critical Rayleigh number R_0 coincides with that one obtained in Banu and Rees (2002). Moreover, in the hypothesis of local thermal equilibrium ($H_0 \to \infty$), by simple calculations, the critical Rayleigh reverts to the classical Rayleigh number for the isotropic porous medium in the local thermal equilibrium (Govender and Vadasz 2007);
(iii) The stabilizing effect of fluid thermal conductivity on the onset of convection is evident since the partial derivative of (29) with respect to η is strictly positive.

4 Nonlinear Stability

In order to study the nonlinear stability of the conduction solution m_0, let us introduce the following Lyapunov functional

$$E(t) = \frac{\|\theta\|^2}{2} + \frac{A\|\phi\|^2}{2\gamma} \tag{30}$$

and define

$$\begin{aligned} D(t) &= \eta\|\nabla_1\theta\|^2 + \|\theta_{,z}\|^2 + \frac{\zeta_1}{\gamma}\|\phi_{,x}\|^2 \\ &\quad + \frac{\zeta_2}{\gamma}\|\phi_{,y}\|^2 + \frac{1}{\gamma}\|\phi_{,z}\|^2 + H\|\theta - \phi\|^2 \\ I(t) &= (\theta, w)\,. \end{aligned} \tag{31}$$

Multiplying $(9)_3$ by θ, $(16)_3$ by ϕ, integrating over V and then adding the resulting equations, we find out

$$\frac{dE}{dt} = -D\left(1 - R\frac{I}{D}\right). \tag{32}$$

In order to capture the influence of rotation on the nonlinear stability analysis of the conduction solution m_0, we shall apply the differential constraint approach (Straughan 2006; Ouarzazi et al. 2017; Capone and Gentile 2018]. To this end, let us consider the following variational problem

$$\frac{1}{R_E} = \max_{\mathcal{H}^*} \frac{I}{D} \tag{33}$$

with

$$\begin{aligned} \mathcal{H}^* = \{(w, \theta, \phi) \ : \ & w = \theta = \phi = 0 \text{ on } z = 0, 1; \text{ periodic in } x \text{ and } y \\ & \text{directions, with period } \frac{2\pi}{a_x}, \frac{2\pi}{a_y} \text{ respectively; } D < \infty; \text{ verifying } (16)_1\} \end{aligned} \tag{34}$$

the space of the kinematically admissible perturbations.

The variational problem (33) is equivalent to

$$\frac{1}{R_E} = \max_{\mathcal{H}} \frac{I + \int_V \lambda\, g\, dV}{D} \tag{35}$$

where $\lambda(\mathbf{x})$ is a Lagrange multiplier and

$$\begin{aligned} g(\mathbf{x}) &= \xi_1 w_{,xx} + \xi_2 w_{,yy} + w_{,zz} + T^2 \xi_1 \xi_2 w_{,zz} - \xi_1 R\theta_{,xx} - \xi_2 R\theta_{,yy} \\ \mathcal{H} &= \{(w, \theta, \phi) \ : \ w = \theta = \phi = 0 \text{ on } z = 0, 1; \text{ periodic in } x \text{ and } y \\ &\qquad \text{directions, with period } \frac{2\pi}{a_x}, \frac{2\pi}{a_y} \text{ respectively; } D < \infty \Big\}. \end{aligned} \tag{36}$$

By applying the Poincaré inequality in $(31)_1$, it turns out that

$$D(t) \geq \pi^2 a \|\theta\|^2 + b\frac{\pi^2}{\gamma}\|\phi\|^2 \tag{37}$$

where

$$a = \min\{\eta, 1\} \qquad b = \min\{\zeta_1, \zeta_2, 1\}. \tag{38}$$

Then, from (32) by virtue of (37) , if $R < R_E$ one obtains:

$$\frac{dE}{dt} \leq \frac{\pi^2 (R - R_E) c}{R_E} E$$

where $c \leq \min\left\{2a, \frac{2b}{A}\right\}$. Hence, the condition $R < R_E$ implies the nonlinear, global and exponential stability of m_0, according to the following inequality

$$E(t) \leq E(0)\ \exp\left[\frac{\pi^2 (R - R_E) c}{R_E}\, t\right]. \tag{39}$$

Remark 2 Multiplying $(9)_1$ by $\mathbf{u}$, integrating over V and applying the Cauchy–Schwarz inequality, it turns out that

$$\delta^{-1} \|\mathbf{u}\|^2 \leq \|\theta\|^2 \tag{40}$$

where $\delta = \frac{R^2}{2} \max\{\xi_1, \xi_2, 2\}$. Therefore, the condition $R < R_E$ implies the decay of $\|\mathbf{u}\|$, as well.

In order to determine the critical Rayleigh number R_E, we solve the variational problem (35). The Euler Lagrange equations are

$$\begin{cases} \theta + \xi_1 \lambda_{,xx} + \xi_2 \lambda_{,yy} + \lambda_{,zz} + T^2 \xi_1 \xi_2 \lambda_{,zz} = 0 \\ 2[\eta \Delta_1 \theta + \theta_{,zz} - H(\theta - \phi)] = \xi_1 R^2 \lambda_{,xx} + \xi_2 R^2 \lambda_{,yy} - Rw \\ \zeta_1 \phi_{,xx} + \zeta_2 \phi_{,yy} + \phi_{,zz} + H\gamma(\theta - \phi) = 0 \\ \xi_1 w_{,xx} + \xi_2 w_{,yy} + w_{,zz} + T^2 \xi_1 \xi_2 w_{,zz} = \xi_1 R\theta_{,xx} + \xi_2 R\theta_{,yy}. \end{cases} \tag{41}$$

By virtue of (20), (41) becomes

$$\begin{cases} \mathcal{L}\mathcal{L}_1\theta = -H\mathcal{L}\phi - R\mathcal{L}w \\ \mathcal{L}w = \xi_1 R\theta_{,xx} + \xi_2 R\theta_{,yy} \\ \mathcal{L}_2\phi = -H\gamma\theta. \end{cases} \tag{42}$$

Applying $\mathcal{L}_2$ to $(42)_1$ and substituting $(42)_2$ and $(42)_3$ in the resulting equation, one obtains (22) and therefore $R_L = R_E$, i.e. the coincidence between the global nonlinear stability threshold and the linear instability threshold, implying the absence of subcritical instabilities. This is an optimal result since the condition $R < R_E = R_L$ is a necessary and sufficient condition to guarantee the stability of m_0.

5 Numerical Simulations

This section will deal with the solution of equation (28). It will be analysed the influence of parameters on the critical Rayleigh number. First of all, we would like to point out the behaviour of function $f_1(\bar{x}, \bar{y})$ in (29). Fixed five parameters $(\xi_1, \xi_2, \zeta_1, \zeta_2, \eta)$ in $f_1(\bar{x}, \bar{y})$, once the following transformation is adopted

$$(\xi_1, \xi_2, \zeta_1, \zeta_2, \eta) \to (\xi_2, \xi_1, \zeta_2, \zeta_1, \eta), \tag{43}$$

values initially assumed by $\bar{x}$ are taken by $\bar{y}$ and vice versa. Moreover, function $f_1(\bar{x}, 0)$ will have the same graph as $f_1(0, \bar{y})$. This behaviour is important because by applying the previous transformation, the same results obtained for $\bar{x}$ hold for $\bar{y}$ and vice versa.

Figure 1 shows the stabilizing effect of rotation on the onset of convection, which is an expected physical behaviour. Moreover, taking into account (29), one immediately proves that $f_1(\bar{x}, \bar{y})$ is an increasing function of $\mathcal{T}^2$. In numerical analysis, for the sake of simplicity, we confine ourselves in considering the case of isotropic porous medium, i.e. $\xi_1 = \xi_2 = \zeta_1 = \zeta_2 = \eta = 1$. However, analogous results are obtained when another set of these parameters is fixed.

Note that in Fig. 1 the critical Rayleigh number is taken as a function of the scaled inter-phase heat transfer coefficient H_0. As Govender and Vadasz (2007) pointed out, since this quantity is not easily measured, we need to determine a range in which this parameter can vary. Starting from its definition $H_0 = \dfrac{h^2 d}{\varepsilon \kappa_z^f \pi^2}$, for reasonable combinations of these param-

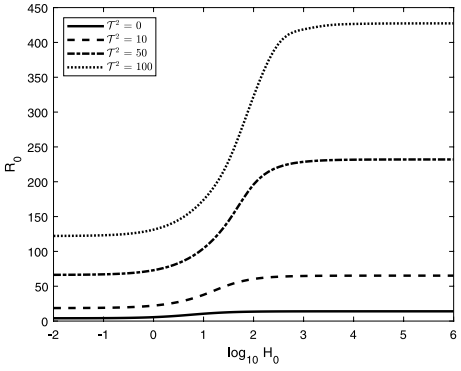

Fig. 1 Critical Rayleigh number as function of the scaled inter-phase heat transfer coefficient H_0 for different values of Taylor number $\mathcal{T}$ with $\xi_1 = \xi_2 = \zeta_1 = \zeta_2 = \eta = 1$ and $\gamma = 0.4$

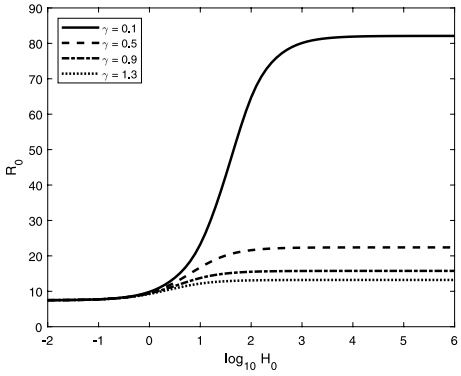

Fig. 2 Critical Rayleigh number as function of the scaled inter-phase heat transfer coefficient H_0 for different values of γ with $\xi_1 = \zeta_1 = 0.1,\ \xi_2 = \zeta_2 = \eta = 1$ and $\mathcal{T}^2 = 20$

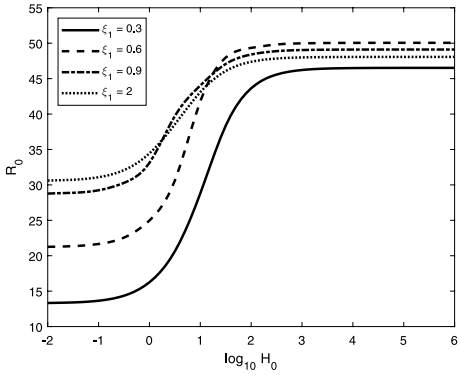

Fig. 3 Critical Rayleigh number as function of the scaled inter-phase heat transfer coefficient H_0 for different values of ξ_1 with $\xi_2 = \zeta_2 = \eta = 1,\ \zeta_1 = 0.1,\ \gamma = 0.4$ and $\mathcal{T}^2 = 20$

eters, H_0 is assumed to vary between 0.01 and 10^6. It is well known that rotation has a stabilizing effect on conduction. In particular, Fig. 1 shows that this effect of Taylor number is very pronounced for large values of H_0, while it is less remarkable for $H_0 \sim 10^{-1}$. We would like to remark that for large values of H_0, each curve tends to become parallel to x axis. As shown in Govender and Vadasz (2007), this behaviour represents the region of local thermodynamic equilibrium and it will characterize the following images, as well.

In Fig. 2, the destabilizing effect of the parameter γ on the onset of convection is clear. For large values of H_0, R_0 is inversely proportional to γ, while for small values of H_0, the presence of γ is negligible. This kind of behaviour is evident in equation (28), and it is reported in Govender and Vadasz (2007), as well. Physically, if h is large, i.e. the heat exchange between the phases is high, increasing the fluid conductivity κ_z^f fosters the onset of convection.

Figure 3 shows the behaviour of the critical Rayleigh number as a function of H_0 for different values of ξ_1. The behaviour for low values of H_0 is similar to the one for large values. In particular, R_0 increases up to a certain value either for $H_0 = 0.01$ and $H_0 = 10^6$. After this point, it starts decreasing toward a limit value. The asymptotic trend is highlighted in Figs 4a, b, where $H_0 = 100$ and $H_0 = 0.01$, respectively.

Furthermore, in Tables 1–2, some significant values of R_0 are reported in order to show which is the critical anisotropy parameter beyond which R_0 inverts its trend, both for $H_0 = 100$ and $H_0 = 0.01$. In addition, note that the moment in which R_0 starts decreasing

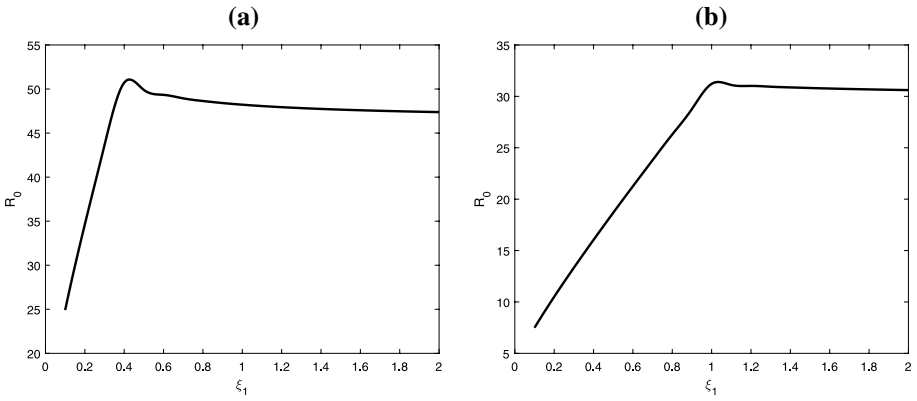

Fig. 4 Critical Rayleigh number as function of ξ_1 with $\zeta_1 = 0.1$, $\zeta_2 = \xi_2 = \eta = 1$, $\mathcal{T}^2 = 20$, $\gamma = 0.4$, **a** $H_0 = 100$, **b** $H_0 = 0.01$

Table 1 Significant values of R_0, $\bar{x}$ and $\bar{y}$ depending on ξ_1, with $\xi_2 = \eta = \zeta_2 = 1$, $\zeta_1 = 0.1$

(a) $H_0 = 100$				(b) $H_0 = 0.01$			
ξ_1	R_0	$\bar{x}$	$\bar{y}$	ξ_1	R_0	$\bar{x}$	$\bar{y}$
0.20	34.6354	0	2.4519	0.80	26.2973	0	4.1436
0.30	43.6359	0	2.9776	0.98	30.7327	0	4.5613
0.39	51.3471	0	3.4167	0.99	30.9769	0	4.5834
0.40	50.7299	7.9758	0	1	31.2207	4.6010	0.0043
0.41	50.6284	7.9648	0	1.01	31.2086	4.6043	0
0.45	50.2671	7.9257	0	1.05	31.1626	4.6001	0
0.50	49.8963	7.8854	0	1.10	31.1098	4.5954	0

Table 2 Significant values of R_0, $\bar{x}$ and $\bar{y}$ depending on ξ_2, with $\xi_1 = \eta = \zeta_1 = 1$, $\zeta_2 = 0.1$

(a) $H_0 = 100$				(b) $H_0 = 0.01$			
ξ_2	R_0	$\bar{x}$	$\bar{y}$	ξ_2	R_0	$\bar{x}$	$\bar{y}$
0.20	34.6354	2.4519	0	0.80	26.2973	4.1436	0
0.30	43.6359	2.9776	0	0.98	30.7327	4.5613	0
0.39	51.3471	3.4167	0	0.99	30.9769	4.5834	0
0.40	50.7299	0	7.9758	1	31.2207	0.0043	4.6010
0.41	50.6284	0	7.9648	1.01	31.2086	0	4.6043
0.45	50.2671	0	7.9257	1.05	31.1626	0	4.6001
0.50	49.8963	0	7.8854	1.10	31.1098	0	4.5954

coincides with the one in which the periodicity cells change their nature. Firstly, when ξ_2 is fixed and ξ_1 is increasing, they are rolls aligned along x axis. Then they turn into rolls aligned along y axis. The opposite transition occurs when transformation (43) is adopted, as shown in Table 2. This phenomenon is physically admissible, as pointed out by Straughan (2019). Small values of ξ_1 imply that the fluid struggles to move in the x direction therefore

Table 3 Significant values of R_0, $\bar{x}$ and $\bar{y}$ depending on ξ_1, with $\xi_2 = \eta = \zeta_1 = 1,\ \zeta_2 = 0.1$

(a) $H_0 = 100$				(b) $H_0 = 0.01$			
ξ_1	R_0	$\bar{x}$	$\bar{y}$	ξ_1	R_0	$\bar{x}$	$\bar{y}$
2.20	86.4714	0	11.3535	0.80	26.2972	0	4.1436
2.30	89.5334	0	11.6095	0.98	30.7327	0	4.5613
2.40	92.5822	0	11.8606	0.99	30.9767	0	4.5834
2.41	92.8864	0	11.8854	1	31.2207	0.0043	4.6010
2.42	96.3788	6.0680	0	1.01	31.2088	4.6043	0
2.43	96.3726	6.0676	0	1.05	31.1628	4.6002	0
2.50	96.3307	6.0649	0	1.10	31.1100	4.5954	0

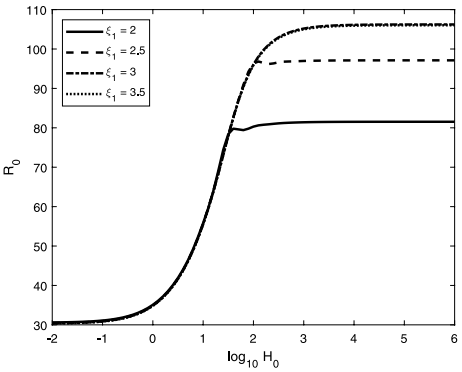

Fig. 5 Critical Rayleigh number as function of the scaled inter-phase heat transfer coefficient H_0 for different values of ξ_1 with $\xi_2 = \eta = \zeta_1 = 1,\ \zeta_2 = 0.1,\ \gamma = 0.4$ and $\mathcal{T} = 20$

the motion has components along y and z axis. Whereas, greater values of ξ_1 allow the fluid to move easier in x direction, favouring the creation of rolls along y axis.

Kvernvold and Tyvand (1979) found that the presence of anisotropic porous media yields a two-dimensional fluid motion. Convective cells are rolls aligned in x or y direction, depending on the ratios between anisotropy parameters. This fluid behaviour is preserved under the hypothesis of local thermal non-equilibrium.

The behaviour of critical Rayleigh number for different values of ξ_1 changes once the ratio $\dfrac{\zeta_1}{\zeta_2}$ is inverted. However, Fig. 5 is similar to Fig. 3.

Increasing ξ_1 makes R_0 grow up to a certain value, beyond which it starts decreasing. Moreover, for small values of H_0, inverting ζ_1 and ζ_2 affects neither the shape of periodicity cells, which are firstly still rolls aligned along x axis, nor the influence of ξ_1 on R_0. Table 3 shows what has been just pointed out.

Now, we decided to fix a direction in which the fluid fails to move easily. So we assumed $\xi_2 = 0.1$ and looked at the critical Rayleigh number as a function of ξ_1. In Fig. 6a, b, the destabilizing effect of permeability is evident, for all H_0, both for $\zeta_1 < \zeta_2$ and $\zeta_1 > \zeta_2$. Recalling the definition of Rayleigh number, this kind of behaviour is expected. Fixed the horizontal permeability parameters K_x and K_y, decreasing values of vertical permeability K_z yield a decrease of Rayleigh number, in agreement with findings of Govender and Vadasz (2007) in the case of horizontal isotropy. Furthermore, increasing K_x will promote the horizontal motion, which increases the preferred cells width and reduces the critical Rayleigh number, as also proposed by Tyvand and Storesletten (1991).

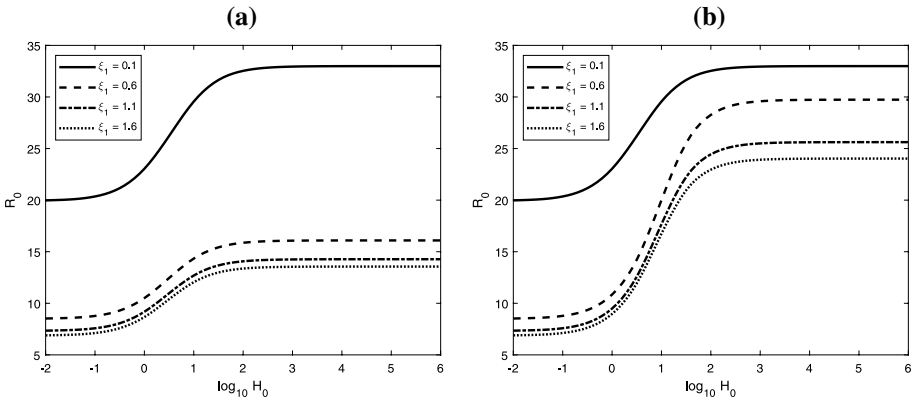

Fig. 6 Critical Rayleigh number as function of H_0 for different values of ξ_1 with $\eta = 1,\ \mathcal{T}^2 = 20,\ \gamma = 0.4$ **a** $\xi_2 = \zeta_1 = 0.1,\ \zeta_2 = 1$, **b** $\xi_2 = \zeta_2 = 0.1,\ \zeta_1 = 1$

Now, let us analyse how R_0 varies with respect to the thermal anisotropy. Figure 7 shows clearly that ζ_1 has a stabilizing effect on conduction if H_0 is large. A similar result is found by Govender and Vadasz (2007) in a simpler situation. Physically, increasing solid conductivity implies that the solid matrix absorbs heat from the fluid more easily. On the other hand, when $H_0 \sim 10^{-1}$, the effect of ζ_1 is negligible.

Tables 4a–b represent a focus on the influence of solid thermal conductivity on the onset of convection. They are obtained when $H_0 = 100$, but however analogous results are valid for all large H_0.

Note that the stabilizing effect of ζ_1 is evident up to a certain value, beyond which R_0 is constant. This behaviour is direct consequence of the change of rolls direction. Once the fluid motion occurs on the plane yz, i.e. rolls are aligned along x axis, modifying ζ_1 does not produce any effect on the motion. Furthermore, inverting the ratio $\dfrac{\xi_1}{\xi_2}$ does not modify the way ζ_1 affects R_0, as shown in Table 4b.

In Fig. 8, the stabilizing effect of fluid thermal conductivity η is highlighted for any H_0. This behaviour is expected since we have shown previously that increasing κ_z^f fosters

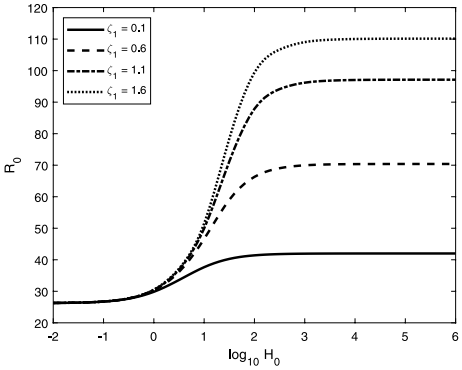

Fig. 7 Critical Rayleigh number as function of the scaled inter-phase heat transfer coefficient H_0 for different values of ζ_1 with $\xi_1 = \eta = \zeta_2 = 1,\ \xi_2 = 0.8,\ \gamma = 0.4$ and $\mathcal{T}^2 = 20$

Table 4 (a) Significant values of R_0 as function of ζ_1 with $\xi_1 = \eta = \zeta_2 = 1,\ \xi_2 = 0.8,\ H_0 = 100$ (b) Significant values of R_0 as function of ζ_1 with $\xi_2 = \eta = \zeta_2 = 1,\ \xi_1 = 0.8,\ H_0 = 100$

(a)				(b)			
ζ_1	R_0	$\bar{x}$	$\bar{y}$	ζ_1	R_0	$\bar{x}$	$\bar{y}$
1.30	95.8271	5.3503	0	0.60	78.6021	6.3297	0
1.31	96.2154	5.3556	0	0.68	82.9496	6.2686	0
1.39	99.2900	5.4055	0	0.69	83.4862	6.2628	0
1.40	99.4132	0	6.2639	0.70	83.7592	0	5.2852
1.41	99.4132	0	6.2639	0.71	83.7592	0	5.2852
1.50	99.4132	0	6.2639	0.80	83.7592	0	5.2852
1.60	99.4132	0	6.2639	0.90	83.7592	0	5.2852

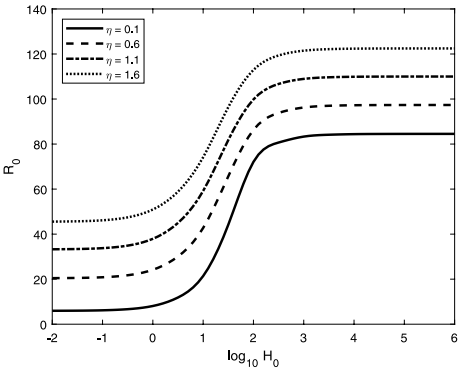

Fig. 8 Critical Rayleigh number as function of the scaled interphase heat transfer coefficient H_0 for different values of η with $\xi_1 = 1.6,\ \xi_2 = \zeta_1 = \zeta_2 = 1,\ \gamma = 0.4$ and $\mathcal{T}^2 = 20$

the onset of convection. Moreover, looking at the definition of R_0 in (28), it is evident that the critical Rayleigh number is directly proportional to η.

6 Conclusions

A linear and nonlinear stability analysis of the conduction solution in a fluid saturating an anisotropic porous layer under the effect of rotation, in local thermal non-equilibrium, has been performed. In particular, the coincidence between the global nonlinear stability threshold and the linear instability threshold has been proved. This means that a necessary and sufficient condition for global nonlinear stability of conduction solution has been obtained. Moreover, we have shown that convection can occur only through a steady motion.

Given that the critical Rayleigh number is obtained in a closed form, we have performed a numerical analysis. We have shown that the increasing conductivity ratio γ has a destabilizing effect on conduction. Mechanical anisotropy ξ_i $(i = 1, 2)$ has the same effect, for ξ_j small $(j \neq i)$, while a slightly different behaviour is obtained when ξ_j is high. Then we have proved that increasing fluid and solid thermal conductivities delay the onset of convection, as well as rotation.

Moreover, the presence of anisotropy forces the fluid in a two-dimensional motion. Convective cells are rolls aligned in x or y direction, depending on the ratios between anisotropy parameters.

Acknowledgements This paper has been performed under the auspices of the National Group of Mathematical Physics GNFM-INdAM. J. Gianfrani would like to thank Progetto Giovani GNFM 2020: "Problemi di convezione in nanofluidi e in mezzi porosi bidispersivi". The Authors would like to thank the anonymous reviewers for their helpful suggestions that led to improvement in the manuscript.

Funding Open access funding provided by Università degli Studi di Napoli Federico II within the CRUI-CARE Agreement.

Declarations

Conflict of interest The authors declare that they have no conflict of interest.

References

Banu, N., Rees, D.A.S.: Onset of darcy-bénard convection using a thermal non-equilibrium model. Int. J. Heat Mass Transfer **45**, 2221–2228 (2002)

Barletta, A.: Routes to Absolute Instability in Porous Media. Springer, Berlin (2019)

Barletta, A., Rees, D.A.S.: Local thermal non-equilibrium analysis of the thermoconvective instability in an inclined porous layer. Int. J. Heat Mass Transf. **83**, 327–336 (2015)

Capone, F., Gentile, M.: Sharp stability results in ltne rotating anisotropic porous layer. Int. J. Thermal Sci. **134**, 661–664 (2018)

Capone, F., Gentile, M., Hill, A.A.: Penetrative convection via internal heating in anisotropic porous media. Mech. Res. Commun. **37**(5), 441–444 (2010)

Capone, F., Gentile, M., Hill, A.A.: Convection problems in anisotropic porous media with nonhomogeneous porosity and thermal diffusivity. Acta applicandae mathematicae **122**(1), 85–91 (2012)

Capone, F., De Luca, R.: Onset of convection for ternary fluid mixtures saturating horizontal porous layers with large pores. Atti della Accademia Nazionale dei Lincei, Classe di Scienze Fisiche, Matematiche e Naturali, Rendiconti Lincei Matematica e Applicazioni **23**(4), 405–428 (2012)

Capone, F., De Luca, R.: Coincidence between linear and global nonlinear stability of non-constant through flows via the rionero "auxiliary system method''. Meccanica **49**(9), 2025–2036 (2014a)

Capone, F., De Luca, R.: On the stability-instability of vertical through flows in double diffusive mixtures saturating rotating porous layers with large pores. Ricerche di Matematica **63**(1), 119–148 (2014b)

Capone, F., De Luca, R.: Porous mhd convection: effect of vadasz inertia term. Transp. Porous Media **118**(3), 519–536 (2017)

Capone, F., De Luca, R.: The effect of the vadasz number on the onset of thermal convection in rotating bidispersive porous media. Fluids **5**(4), 173 (2020)

Capone, F., De Luca, R., Gentile, M.: Thermal convection in rotating anisotropic bidispersive porous layers. Mech. Res. Commun. **110**, 103601 (2020b)

Capone, F., Rionero, S.: Brinkman viscosity action in porous mhd convection. Int. J. Non-Lin. Mech. **85**, 109–117 (2016a)

Capone, F., Rionero, S.: Porous mhd convection: stabilizing effect of magnetic field and bifurcation analysis. Ricerche di Matematica **65**(1), 163–186 (2016b)

Capone, F., De Luca, R., Gentile, M.: Coriolis effect on thermal convection in a rotating bidispersive porous layer. Proc. Royal Soc. A: Math. Phys. Eng. Sci. **476**(2235) (2020a)
Celli, M., Barletta, A., Rees, D.A.S.: Local thermal non-equilibrium analysis of the instability in a vertical porous slab with permeable sidewalls. Transp. Porous Media **119**(3), 539–553 (2017)
Chandrasekhar, S.: Hydrodynamic and hydromagnetic stability. Courier Corporation, USA (2013)
Franchi, F., Lazzari, B., Nibbi, R., Straughan, B.: Uniqueness and decay in local thermal non-equilibrium double porosity thermoelasticity. Math. Methods Appl. Sci. **41**(16), 6763–6771 (2018)
Gentile, M., Straughan, B.: Structural stability in resonant penetrative convection in a forchheimer porous material. Nonlin. Anal: Real World Appl. **14**(1), 397–401 (2013)
Gentile, M., Straughan, B.: Bidispersive vertical convection. Proc. Royal Soc A: Math. Phys. Eng. Sci. **473**(2207), 20170481 (2017)
Govender, S.: Coriolis effect on the stability of centrifugally driven convection in a rotating anisotropic porous layer subjected to gravity. Transp. Porous Media **67**(2), 219–227 (2007)
Govender, S., Vadasz, P.: The effect of mechanical and thermal anisotropy on the stability of gravity driven convection in rotating porous media in the presence of thermal non-equilibrium. Transp. Porous Media **69**, 55–66 (2007)
Hema, M., Shivakumara, I.S., Ravisha, M.: Double diffusive ltne porous convection with cattaneo effects in the solid. Heat Transf. **49**(6), 3613–3629 (2020)
Kuznetsov, A.V., Nield, D.A., Barletta, A., Celli, M.: Local thermal non-equilibrium and heterogeneity effects on the onset of double-diffusive convection in an internally heated and soluted porous medium. Transp. Porous Media **109**(2), 393–409 (2015)
Kvernvold, O., Tyvand, P.A.: Nonlinear thermal convection in anisotropic porous media. J Fluid Mech **90**, 609–634 (1979)
Malashetty, M.S., Shivakumara, I.S., Kulkarni, S.: The onset of convection in an anisotropic porous layer using a thermal non-equilibrium model. Transp. Porous Media **60**, 199–215 (2005)
Nield, D.A., Bejan, A.: Convection in Porous Media. Springer, Berlin (2017)
Nield, D.A., Kuznetsov, A.V.: The onset of convection in an anisotropic heterogeneous porous medium: a new hydrodynamic boundary condition. Transp. Porous Media **127**(3), 549–558 (2019)
Ouarzazi, M.N., Hirata, S.C., Barletta, A., Celli, M.: Finite amplitude convection and heat transfer in inclined porous layer using a thermal non-equilibrium mode. Int. J. Heat Mass Tran. **113**, 399–410 (2017)
Storesletten, L.: Effects of anisotropy on convection in horizontal and inclined porous layers. Emerg. Technol. Tech. Porous Media **134**, 285–306 (2004)
Storesletten, L., Rees, D.A.S.: An analytical study of free convective boundary layer flow in porous media: the effect of anisotropic diffusivity. Transp. Porous Media **27**, 289–304 (1997)
Straughan, B.: Global nonlinear stability in porous convection with thermal nonequilibrium model. Proc. R. Soc. A **462**, 409–418 (2006)
Straughan, B.: Stability and wave motion in porous media, vol. 165. Springer, Berlin (2008)
Straughan, B.: Porous convection with local thermal non-equilibrium temperatures and with cattaneo effects in the solid. Proc. Royal Soc A: Math, Phys. Eng. Sci. **469**(2157), 20130187 (2013)
Straughan, B.: Convection with Local Thermal Non-equilibrium and Microfluidic Effects. Springer, Berlin (2015)
Straughan, B.: Anisotropic bidispersive convection. Proc. Royal Soc. A: Math. Phys. Eng. Sci. **475**(2227) (2019)
Tyvand, P.A., Noland, J.K.: Laterally penetrative onset of convection in a horizontal porous layer. Transp. Porous Media **134**(1), 77–95 (2020)
Tyvand, P.A., Storesletten, L.: Onset of convection in an anisotropic porous medium with oblique principal axes. J. Fluid Mech. **226**, 371–382 (1991)
Tyvand, P.A., Storesletten, L.: Onset of convection in an anisotropic porous layer with vertical principal axes. Transp. Porous Media **108**(3), 581–593 (2015)
Vadasz, P.: Coriolis effect on gravity-driven convection in a rotating porous layer heated from below. J. Fluid Mech. **376**, 351–375 (1998)
Vadasz, P.: Heat transfer and fluid flow in rotating porous media In Developments in Water Science. Elsevier, Amsterdam (2002)
Vadasz, P.: Fluid flow and heat transfer in rotating porous media. Springer, Berlin (2016)
Vadasz, P.: Instability and convection in rotating porous media: a review. Fluids **4**(3), 147 (2019)